15 Years of Comet Photometry : A Comparative Analysis of 80 Comets

David J. Osip, David G. Schleicher, Robert L. Millis

Lowell Observatory

Michael F. A'Hearn

University of Maryland

Peter V. Birch

Perth Observatory

In 1976 we began a program of narrowband photometry of comets that has encompassed well over 400 nights of observations. To date, the program has provided detailed information on 80 comets, 11 of which have been observed during multiple apparitions. The filters (initially isolating CN, C_2, and continuum and later including C_3, OH, and NH) as well as the detectors used for the observations were changed over time, and the parameters adopted in the reduction and modelling of the data have likewise evolved. Accordingly, we have re-reduced the entire database and have derived production rates using current values for scalelengths and fluorescence efficiencies. Having completed this task, the results for different comets can now be meaningfully compared. General characteristics we will discuss in this paper include ranges in composition (molecular production rate ratios) and dustiness (gas production compared with $Af\rho$). Additionally, we will present an analysis of trends focusing on how the production rates vary with heliocentric distance and on pre- and post-perihelion asymmetries in the production rates of individual comets. Possible taxonomic groupings will also be described. This research is supported by a grant from the NASA Planetary Astronomy Program.

Delivery of Meteorites from the Asteroid Belt.

M. Nolan and R. Greenberg / University of Arizona

The study of asteroid formation and composition is of keen interest, since the processes that formed our own Earth and the other planets may have been similar in some important ways. Also, the numerous objects in the main asteroid belt and elsewhere help us avoid the "sample of one" problem so common in planetary science. Unfortunately, asteroids are very difficult to study directly: we have relatively noisy, low resolution optical spectra of their disk-averaged surfaces in reflected sunlight or thermal emission, and even then we see only their "dirty" surfaces. Meteorites, on the other hand, can be studied in great detail at high resolution by a wide array of techniques with much lower noise. Thus it would aid our understanding to know how asteroids and meteorites are connected, even if only statistically.

Transport processes for bringing asteroids from the asteroid belt to the Earth have been critically reviewed by Greenberg and Nolan [1989]. Wisdom [1983] and Froeschlé and Scholl [1986] have shown that asteroidal material may be transported to the Earth by way of Jovian and secular resonances. We do not know for certain how asteroids get into the resonances, which are now fairly clear of asteroids, probably due to the same processes that bring material to the Earth. We probably understand in general the dynamical delivery mechanisms, but not their relative efficacy, or what regions of space they sample.

The main belt size distribution is known for sizes $\gtrsim 30$ km in diameter by direct telescopic observation, with some extrapolation and bias corrections for albedo at the smaller sizes. However, collisions are most likely to occur with smaller bodies. Thus our estimates for the collisional lifetimes of the bodies we can see are very uncertain. The collisional lifetimes affect in turn the expected steady-state population of bodies at all sizes.

As an alternative to using a variety of poorly understood processes to analyze the meteorite delivery process from the main belt, we can look at the process from the other end: meteorites arriving at the Earth. Networks of cameras operating since the early 1950s (*cf.* Jacchia and Whipple [1961]) photographed several thousand meteor trails. From these photographs, it was possible to determine the orbits of the asteroids which fell as meteors. Wetherill and ReVelle [1981] chose 27 meteors which they believed to be of ordinary chondritic composition (including Lost City, a recovered meteorite). Their orbital elements in a, e space show clusters near several Jovian resonances zones. We have similarly examined the orbits of 42 496 meteors from the IAU Meteor Data Center. Clustering persists only weakly in the vast data. The low accuracy of many of the orbits (D. Steele, pers. comm.) is a critical factor. There is a strong clustering toward orbits with perihelia near 1 AU. The Öpik two-body treatment of the the gravitational attraction of the Earth may not be sufficient for these orbits. We are numerically integrating the orbits of these meteors, to determine how large a correction is required. These results will help constrain how many came to Earth-crossing by each of the possible routes.

A NEW METHOD FOR ASTROMETRIC OBSERVATIONS OF ASTEROIDS

Th. Pauwels, *Koninklijke Sterrenwacht van België, Ringlaan 3, B-1180 Brussel, Belgium*

When no accurate positions are known, on astrographic plates asteroids reveal themselves among the stars by their motion only. Therefore astrographic observations of asteroids are always done in such a way that moving objects can easily be detected on the plates. Among the classical methods we may mention:

- Long exposures, such that moving objects show trails.
- Long exposures with interruptions, such that moving objects give several images. The interruptions can be symmetric or asymmetric.
- Several plates of the same field with a small separation in time. Moving objects are detected by blinking the plates.
- Several exposures on the same plate, shifted by a known amount. Moving objects reveal themselves by a different pattern formed by the different exposures.

The method we suggest here consists of several superimposed so-called Trepied-Metcalf exposures. Each of the exposures is guided with the average (or expected) motion of the target objects. By superimposing several exposures, stars will show only one (trailed) image, while moving objects will show several images (more or less trailed, depending from how much each object's motion differs from the introduced average motion).

This method has several advantages over the classical methods. Some of these are:

- Fainter limit magnitude thanks to the Trepied-Metcalf exposure.
- No overloading of the picture, since there is only one image per star.
- Very easy detection of moving objects, not requiring a blink comparator.
- More precision in the measurements of the moving objects by measuring all images. Yet there is no need to measure several images of the reference stars.
- No waste of time between the exposures (compared to the second described classical method).

A few disadvantages are:

- Accumulation of sky background because of several exposures on the same plate.
- Very large non-spherical reference stars.
- Although possible, finding the motion of an object for recovery on following nights is difficult.
- Only one astrometric position for several images, all to be measured, since the distance between the exposures is *not* the motion of the object, but the manually introduced motion in guiding.

All these advantages and disadvantages can also be found in one or more classical methods. The desired combination of advantages and disadvantages should guide the observer in choosing his favourite method.

THE IMPORTANCE OF GUIDING ON THE MOTION OF A COMET IN ASTROMETRIC OBSERVATIONS

Th. Pauwels, *Koninklijke Sterrenwacht van België, Ringlaan 3, B-1180 Brussel, Belgium*

When doing astrometric observations of a comet, one is not interested in a beautiful picture, nor in showing the tail of a comet. Often, it may seem unnecessary to guide on the motion of the comet. A plate guided on the motion of the stars and with a trailed image of the comet can look very acceptable to be measured for an astrometric position. However, the results obtained in this way will be wrong.

When observing for an astrometric position, one is interested in the nucleus of the comet. This one can never be observed. However, the central condensation gives a very good approximation of the position of this nucleus. One tries to find the maximum of the light distribution of the cometary image and to take that as the position of the comet (the images of the Giotto spacecraft have shown that this introduces an error of the order of 10-20 km, which is completely negligible). In reallity the eye will not point the maximum but the middle of some isophote surrounding this maximum closely.

If the comet has moved (say, perpendicularly to the direction of the tail) during the exposure, then it may look as if there is a trailed central condensation, which can be measured quite well. However, positions obtained in this way will be shifted towards the tail of the comet, thus introducing a systematic error in the positions. This is due to the fact that the light intensity at any point of the photographic plate will be the integral of the light intensity of the comet, integrated along a line parallel to its motion. This integral will be a function of only one coordinate (perpendicular to the motion of the object), and will have a maximum for a different value of that coordinate than the original function. Usually the light distribution along a line parallel to the motion will have a rather sharp maximum if the cut is through the central condensation, but more prominent wings if the cut is shifted towards the tail. These wings can contribute more to the total integrated light distribution and thus give a brighter image than at the real location of the central condensation.

On LAMs and SAMs for Halley's Rotation

S. J. Peale
Dept. of Physics
University of California
Santa Barbara, CA

Both Long axis modes (LAMs) and short axis modes (SAMs) have been proposed for Halley's comet, where the acronyms refer to non principal axis rotation with precession of the spin vector in the body frame of reference about the axes of minimum moment of inertia and maximum moment of inertia respectively. The non principal axis rotation is invoked to accommodate a dual periodicity in the light curves, jet shapes and other types of observations of the comet. A LAM is characterized by a rotation of the long axis of the nucleus about the spin angular momentum vector with period P_ϕ while the nucleus rotates about the long axis with period P_ψ, which is the period of precession of the rotation vector about the long axis in the body frame of reference. The long axis also nods with a period of $P_\psi/2$ but with small amplitude for Halley's shape. The rotation of the long axis about the angular momentum vector with period P_ϕ as the long axis nods also is characteristic of a SAM, but in this case the motion *about* the long axis is an oscillation with period P_ψ instead of a complete rotation. Both Belton *et al.* (1991) and Samarasinha and A'Hearn (1991) find that only a LAM with $P_\phi \approx 3.7$ days and $P_\psi \approx 7.1$ to 7.4 days can be consistent with an extensive list of observational constraints. On the other hand, there can be no "Springtime for Halley" for a LAM to account for the post perihelion brightening of the the comet without an additional degree of freedom such as activating a new jet at perihelion passage at each apparition. All parts of the nucleus receive full solar illumination during the rotation cycle at all parts of the orbit for a LAM. The maximum rate of emission of a jet source is then governed only by Halley's proximity to the Sun leading to a light curve that is symmetric about perihelion if thermal inertia effects are small. For a SAM, the motion of the nucleus about the long axis is limited to a relative small range of angles, so with an appropriate orientation of the spin angular momentum with significant obliquity to the orbit plane, an active source could remain more or less in shadow until after perihelion passage to account for the post perihelion brightening. Since the post perihelion brightening is a robust observation of every apparition, whereas some of the other constraints depend on uncertain model parameters, it would appear that any derived rotation state must first be able to account for the post perihelion brightening. Either the LAM must be embellished to account for the brightening by some effect perhaps involving thermal inertia, or a SAM must be found that will remain consistent with the observations that have so far eliminated it. Halley's persistent activity at large post perihelion distances and the recent outburst of its cold nucleus may provide clues to a means for storing solar energy in a LAM nucleus.

COMET CLOSE ENCOUNTERS AND HYPERBOLIC METEOROIDS;
E.M.Pittich, Astronomical Institute, Slovak Academy of Sciences, 842 28 Bratislava, Czechoslovakia.

Catalogues of meteor orbits contain some quantity of hyperbolic orbits. In spite of the large percentage of these orbits is evidence that hyperbolic orbits are the result of measuring errors, some of them are real nonperiodical orbits. Part of hyperbolic orbits can be originated from cometary meteoroids at close encounters to the giant planets. This result was obtained by the numerical integration of orbits of meteoroids, which were ejected from nuclei of comets P/Shajn-Schaldach, and P/Encke, respectively. The first of these comets represents comets with close encounters to the planets during their orbital evolution, the second comet is the typical example of a comet without close encounters.

CHARACTERISTICS OF THE 1969 LEONIDS AND 1982 LYRIDS BURSTS; V. Porubčan and J. Štohl, Astronomical Institute SAV, 84228 Bratislava, ČSFR

Radar observations of the last bursts of the Leonids (1969) and Lyrids (1982) carried out at the Springhill Meteor Observatory, Canada, have enabled a detailed study of the activity and mass distribution of meteoroids across the corresponding dense and relatively young filaments of the two meteor streams. A significant common feature of both bursts is their very short duration, with the rates exceeding a half-maximum rate within 15-20 minutes only, and those exceeding a quarter-maximum rate within 50-55 minutes. Mass distribution exponent of the meteoroids in the filaments largely differs from the values obtained for the older populations of the streams. The highest mass exponent s 2.2 - 2.4 is found around the peak of the activity, confirming high contribution of smaller meteoroids in the narrow filaments of recent origin. Origin of the filaments in both streams is discussed.

THE FLUX OF SMALL ASTEROIDS NEAR THE EARTH; D. L. Rabinowitz, Lunar and Planetary Laboratory, The University of Arizona, Tucson AZ 85721

Until recently, no asteroid smaller than 100m had ever been identified outside the Earth's atmosphere. Such objects had been observed only as bright meteors and fireballs, with estimated diameters rarely exceeding 10m. Since September of 1990, however, T. Gehrels, J. V. Scotti, and I have made astrometric observations of two objects, 1990 UN and 1991 BA, with estimated diameters of 90 and 9m, respectively. These were discovered in the course of a regular search for Earth-approaching asteroids which we conduct each month at the 0.91m Spacewatch Telescope on Kitt Peak. We use a TK2048 CCD in drift-scan mode to image the sky and a real-time computer to monitor, record, and analyze the data. Our average discovery rate is about two Earth approachers per month, with absolute magnitudes ranging from 14.5 to 28.5. In this paper, I use these observations and also a computer model of the asteroid population observable by the Spacewatch Telescope to determine the asteroid flux near the Earth as a function of absolute magnitude. The computer model is necessary in order to determine the efficiency of the Spacewatch Telescope for detecting Earth approachers as a function of their size, phase angle, angular rate, and distances to the sun and the Earth. Given an assumed magnitude distribution, the model allows me to compute the expected number of Spacewatch discoveries as a function of absolute magnitude. I find that for asteroids larger than 100m, the observed magnitude dependence is consistent with the cumulative magnitude-frequency relation established for the main belt asteroids. Assuming this relation extends to smaller sizes, however, the probabilities for discovering 1990 UN and 1991 BA are only 10% and 1%, respectively. Objects smaller than 100m are therefore increasingly overabundant compared to an extrapolation from larger objects, with this excess increasing with decreasing size. Near 10m, the most probable flux near the Earth is two orders of magnitude higher. This is in agreement with the fluxes estimated from observations of bright meteors and fireballs. It is likely that processes other than collisional breakup of asteroidal material begin to supply the population of small objects near the Earth at sizes near 100m.

The 16 March 1986 Disconnection Event in Comet Halley

C.E. Randall, J.C. Brandt and Y. Yi
(U. Colorado/LASP)

We present an analysis of a disconnection event (DE) in Comet Halley in mid-March of 1986. Although disconnection events are arguably the most spectacular of all dynamic comet phenomena, the mechanisms by which they occur are not fully understood. It is generally believed that the solar wind plays a major role in determining when disconnection events occur, but the details of the solar wind/cometary interactions responsible for initiating the tail disconnection are still under debate. The two most widely accepted models are (1) high speed streams in the solar wind cause the tail to disconnect through such mechanisms as increased ion production or pressure effects; and (2) the tail disconnects after frontside reconnection of the interplanetary magnetic field (IMF) as the comet crosses a magnetic field sector boundary.

In order to study these proposed mechanisms, we have analyzed photographs from the International Halley Watch (IHW) archive throughout the 1985-1986 Comet Halley appearance. Photos between 16 March 1986 and 19 March 1986 clearly show the occurrence of a disconnection event, which we discuss here. From the images we have determined the precise time of the DE, and have examined the solar wind conditions and interplanetary magnetic field at this time in order to ascertain whether any correlations were evident which would support one of the proposed mechanisms for DE occurrence.

From kinematic extrapolation of tail–nucleus distance measurements on the photographs, we calculated the disconnection time of the 16-19 March 1986 event to be 16.1 ($\pm$0.1) March. We inferred the solar wind conditions around Comet Halley by corotating data from the IMP-8 satellite to the comet. Using this data, we determined that at the time of the DE the solar wind speed at the comet was $\sim$ 600 km/sec; the solar wind density was $\sim$ 8 cm^{-3}; and the IMF magnitude was $\sim$ 8 nT. These conditions are not particularly unusual, and thus would *not* be expected to have caused the observed DE via mechanisms such as ion production or pressure effects.

We estimated the position of the IMF neutral sheet using two different methods. The times and positions of 180-degree phase shifts in the IMF direction were measured by the IMP-8, ICE and PVO satellites, and corotated to Comet Halley's orbit. Also, the neutral sheet calculated at the solar source surface was corotated out to the comet. Both methods are consistent with one another, and show that Comet Halley crossed a magnetic field sector boundary shortly before the 16 March DE. We therefore conclude that the most likely cause of this disconnection event was front-side reconnection of the IMF.

Laboratory Studies On Cometary Crust Formation: The Importance Of Sintering; L. Ratke, H. Kochan, H. Thomas, Institut für Raumsimulation, DLR-Köln, P.O. Box 906058, D-5000 Köln 90, FRG.

In laboratory simulations with porous water-ice-dust mixtures strong crusts are observed after insolation with an artificial sun. Within the KOSI project strength increases up to an order of magnitude were observed compared to the strength of the loosely packed ice-dust mixtures. In the KOSI-experiments it was found that the thickness of the crust depends on the insolation power, its duration, the temperature profile, and the composition of the ice-dust mixture [1].The mechanism of crust formation are still unknown in detail. One of the mechanisms under discussion is the recondensation of the inward diffusing volatiles. This would reduce the pore volume and thus strengthen the ice-dust body. We propose here two other mechanisms which maybe of general importance especially for real comets: sintering of loosely packed ice-dust particles either due to sublimation and condensation or due to surface diffusion. Solid state sintering of particles is a well known phenomenon in powder metallurgy [2,3]. Sintering - which means the densification of arbitrarily packed powder aggregates - occurs due to dependence of for instance the partial pressure of water on particle radius or more generally the dependence of the chemical potential of a species on the particle curvature. The sintering process within particle aggregates forms "sinter necks" at the contact points between the particles. These have lower partial pressure than adjacent spherical particles. The neck grows therefore by transport of sublimated water from points of higher to lower curvature. Applying the theories developed in powder metallurgy to ice aggregates it is possible to describe the crust formation and its increasing strength. At different homologous temperatures different transport mechanisms (sintering) may occur.
At temperatures above 200 K sintering due to sublimation and condensation is possible, whereas at lower temperatures surface diffusion gives a faster reduction of pore volume and thus an increase in strength. The theoretical discussion of the crust formation by sintering supplemented by laboratory investigations performed with pure ice at different temperatures.

[1] H.Kochan,K.Roessler,L.Ratke,M.Heyl,H.Hellmann, G.Schwehm, *Proc. Int.Workshop on Physics and Mechanics of Cometary Materials*, MÜnster,FRG 1989, ESA-SP-302, pp.115-119
[2] H.E.Exner, *Principles of Single Phase Sintering*, Rev. Powder Met. Phys.Ceram.,1979, Vol.1, pp.7-251
[3] G.C.Kuczynski, *Physics and Chemistry of Sintering*, Advanc. Colloid Interf.Sci.,1972, vol.3, pp.275-330

VELOCITIES IN THE H_2O^+-ION TAIL OF COMET LEVY 1990c

H. Rauer, K. Jockers, C. Debi-Prasad, Max-Planck-Institut für Aeronomie,
D-W-3411 Katlenburg-Lindau, Germany

E.H. Geyer, Observatorium Hoher List, D-W-5568 Daun, Germany

Comet Levy 1990c was observed at the Observatory Hoher List, FRG, from 16th to the 25th of August 1990. A focal reducer and the CCD-camera of the Max-Planck-Institut für Aeronomie were used. The field of view was approximately 25 arcmin. Images were taken through an interference filter at 615.8±1.8 nm, to observe the H_2O^+-ion tail. The dust continuum was observed through another filter of 3 nm FWHM centered at 642 nm. From these images column densities have been derived out to a distance of 1 10^6 km from the cometary nucleus. Interferograms, using a Fabry-Perot-etalon with a fixed gap of 0.9 mm and spectral resolution of 0.2 Å at 615.8 nm, were also taken. From these interferograms, the geocentric velocity component of the water ions in the plasma tail has been derived. 2-dimensional velocity maps will be presented. These were used, together with the column densities derived in the images taken before and after the interferograms, to calculate production rates.

Space Weathering of a Non-Spherical, Rotating Body, R. O. Redman, National Research Council of Canada

During cratering events on airless bodies, large numbers of small particles are blasted out of the surface, with small particles generally having higher speeds than large particles. If the parent body is non-spherical and rotating, it can exchange energy gravitationally with the ejected particles. Some low energy particles are boosted into escaping orbits, while other high energy particles are recaptured. This process has been modelled for a contact binary asteroid consisting of two touching spheres rotating about their centre of mass at a specified fraction of the breakup velocity. The domain of initial velocities for which an ejected particle is recaptured has a fractal structure. The author hopes to illustrate this using an interactive computer program which calculates the orbit corresponding to each initial velocity. The implications for the collection of dust and gravel in the regolith of a rotating, non-spherical asteroid will be discussed.

VISUAL DATA OF MINOR METEOR SHOWERS

J. Rendtel, Arbeitskreis Meteore, PSF 37, 1561 Potsdam, Germany
International Meteor Organization

There are different lists of meteor showers, partially containing hundreds of radiants. Even if these would represent real sources of meteoroids, an observer cannot associate meteors seen to all these radiants.

The Visual Commission of the *International Meteor Organization, IMO* formulated rules for the work of visual observers. Three essential information which can be obtained by well trained observers are considered for shower association of meteors:

(i) direction of the trail (tracing back the line must meet the radiant of a certain size)

(ii) apparent trail length must not be longer than half the distance from its (possible) radiant; exception: fireballs penetrating to lower end heights

(iii) the angular velocity in dependence on the meteor's elevation and its distance from the radiant

In order to distinguish shower meteors from different showers as well as from the sporadic background, the observer is forced to look not more than 40° away from the radiant(s) under study. Furthermore, a radiant should be situated at least 30° above horizon. Otherwise the correction to zenith position becomes too large and the result is then uncertain simply due to the reduced number of shower meteors visible.

A mathematical treatment of the pollution of shower rates only by accidentially aligned sporadic meteors by GYSSENS (1989) yields to a rate of about 2/hour.

Experimental data derived from observational material of end August led to a ZHR of about 2 ... 3 for arbitrary points at the sphere fulfilling the above mentioned criteria. More recent analyses of spring data at a lower meteor activity level confirm, that one may expect a rate of about 15 percent of the total rate from any assumed radiant of about 10° diameter. If a certain velocity is assumed, this rate decreases to less than 10 percent for experienced observers.

Consequently, an experienced observer considering all the three criteria mentioned in the beginning, may deliver useful ZHR-values as soon as the ZHR reaches 2.5 ... 3. All ZHR below this level must be regarded as insignificant and useless.

The IMO collects visual observations in its Visual Meteor DataBase (VMDB). It contains statistical data of about 100,000 meteors per year and allows calculations of ZHR as well as of the population index r (or the mass index s). Knowing these data, further quantities, such as the number density or the particle flux can be determined (RENDTEL and KOSCHACK, 1989 and 1990).

In the IMO working list of showers are included only showers

(i) reaching a certain level of activity, and

(ii) having known orbital elements (thus known geocentric velocity).

All other meteors are regarded to be sporadic. Since the meteor trails are plotted on gnomonic charts (except the periods of high activity near major shower maxima), searches for radiants being of interest later, can be done. Furthermore, IMO prepares a positional database (PosDat). It will contain positional data of visual and telescopic meteors and is connected with a radiant search program. This will allow an effective search for instance for a possible activity of asteroid related radiants.

OBSERVED SPATIAL PROFILES OF C_2, C_3, CH, CN, [OI] AND NH_2 IN COMETS HALLEY, WILSON AND NISHIKAWA-TAKAMIZAWA-TAGO

Terrence W. Rettig (University of Notre Dame and Arizona State University)
Susan Wyckoff, Rodney S. Heyd (Arizona State University) and Raylee Stathakis (Anglo-Australian Observatory) and D. A. Ramsay (Herzberg Institute of Astrophysics, NRCC)

Long-slit spectral observations of comets Halley (1986), Wilson (1987) and Nishikawa-Takamizawa-Tago (1987) were obtained with the 3.9 meter Anglo-Australian Telescope. The observations of P/Halley were obtained in April 1986 and observations for C/Wilson and Nishikawa-Takamizawa-Tago were obtained in May 1987. Spectra of comets Halley and Wilson were obtained with the IPCS at a spectral resolution of 0.5 A and a spatial resolution of 10^3 km. Also, spectra of comets Wilson and Nishikawa-Takamizawa-Tago were obtained with a CCD at a resolution of 1.5 A and a spatial resolution of approximately $3x10^3$ km. The measured surface brightness profiles extend to approximately $6x10^4$ km from the nucleus in both sunward and tailward directions. Spatial profiles for C/Wilson are compared at the two different spectral resolutions with the IPCS and CCD detectors. These three comets were at approximately the same heliocentric distances and the brightness profiles are shown to have the same shapes within the observed errors even though the gas/dust ratios vary appreciably. Hence, the scalelengths derived from spatial profiles are determined to be the same for identical molecules in each of the three comets suggesting these molecules are derived from common parents. Production rates for NH_2 are determined and NH_2/H_20 ratios are presented. With standard parameters, the NH_2 brightness profile fits the vectorial model, reaffirming the probable NH_3 parenthood.

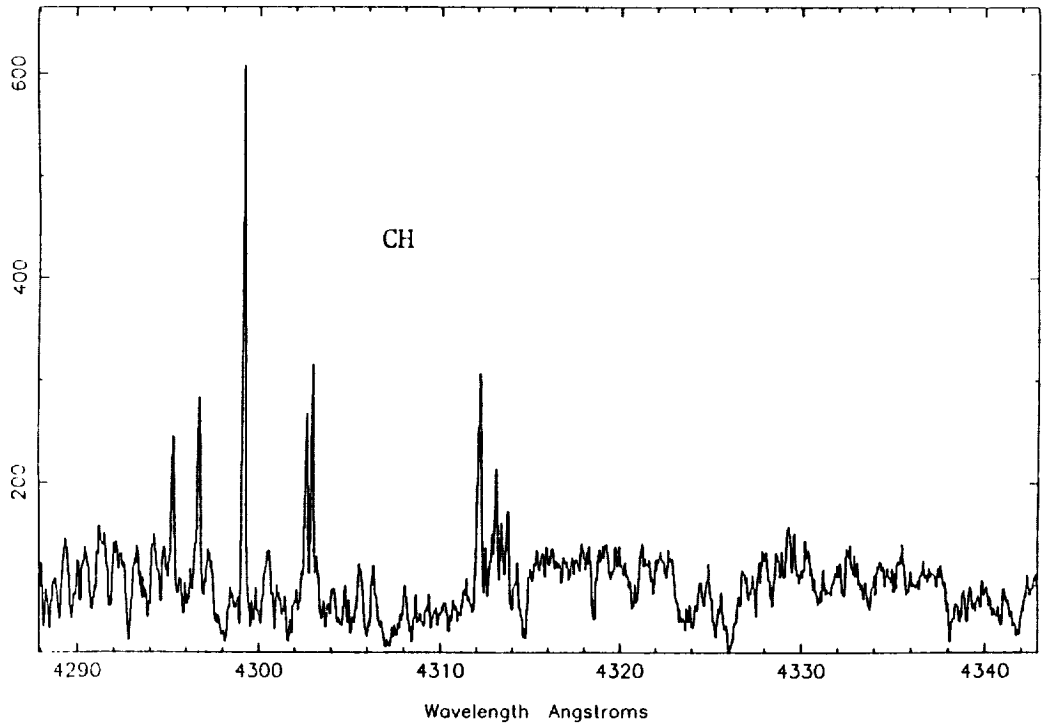

PARENT MOLECULAR SCALELENGTHS INFERRED FROM THE OBSERVED SURFACE BRIGHTNESS DISTRIBUTIONS OF C_2, C_3, NH_2, CH, CN, AND [OI] IN COMETS

Terrence W. Rettig (University of Notre Dame and Arizona State University),
Susan Wyckoff, Rodney S. Heyd, and Lisa Engel (Arizona State University)

Of the five molecules commonly observed in ground-based spectra of comets, the parent of only one species, NH_2, has been tentatively identified (NH_3). All radicals observed in the fluorescence spectra of comets are probably photodissociation fragments of parent molecules released directly from the comet nucleus. Thus with an appropriate coma outflow model and radical photodissociation timescale, the scalelength of a parent molecule can be inferred from the observed spatial distributions. Long-slit spectral observations of comets Halley, Wilson and Nishikawa-Takamizawa-Tago were obtained with the 3.9-m Anglo-Australian Telescope. The spectrograph slit in each case was centered on the comet nucleus and aligned with the comet tail axis. Spatially resolved surface brightness profiles of each molecular species were extracted from the long-slit spectra for each comet using IRAF routines. Empirical *vectorial* parent scale lengths were determined by matching the column densities predicted using the vectorial model (Festou 1981) to the observed spatial profiles. Photodissociation timescsales for candidate parent molecules of the observed species C_2, C_3, NH_2, CH, CN, and [OI] were calculated, and together with the model fits to the observed profiles, were used to infer possible parent identities.

RESONANCE FLUORESCENCE EXCITATION OF THE CN B-X(0,0) AND (0,1) P AND R BRANCHES IN COMET HALLEY

Terrence W. Rettig (University of Notre Dame and Arizona State University) and Marvin Kleine (Arizona State University) and D. A. Ramsay (Herzberg Institute of Astrophysics, NRCC)

High resolution spectra (0.5 A) of the P and R branches of the CN(0,0) violet system at 3883 A and the CN(0,1) band at 4216 A are presented. The spectra were obtained for comet P/Halley on 15 May 1986, when r = 1.38 A.U. and Δ = 0.43 A.U., using the 3.9-m Anglo-Australian Telescope. The P and R branch rotational lines in the two CN bands show the expected identical structure and internal relative intensities due to the fact that both bands originate from the same upper vibrational level in the B state. Spatial profiles are also presented for the CN(0,0) and CN(0,1) bands covering the sunward and tailward directions. These profiles show a noticeable variation in the log-log slope that cannot be explained or accounted for by stimulated emission, self-absorption, collisions or a contaminant. The rotational structure of the CN bands was modelled using a full fluorescence calculation of the lower three electronic states of the CN radical (A,B,X). The predicted rotational line intensities compare very well with the observations for both bands: CN(0,0) and CN(0,1).